He. 2. 3. 06

Longitudinal EAS Development at $E_0 = 10^{18} - 3 \cdot 10^{19}$ eV and the QGSJET Model

S.P.Knurenko[1], V.R.Sleptsova[1], I.Ye.Sleptsov[1], N.N.Kalmykov[2], S.S.Ostapchenko[2]

[1] *Institute of Cosmophysical Research and Aeronomy, 31 Lenin Ave., 677891, Russia*

[2] *Institute of Nuclear Physics of Moscow State University, Moscow, 119899, Russia*

Abstract

The longitudinal shower development in the energy range of $10^{18} - 3 \cdot 10^{19}$ eV by using correlation parameters N_s and Q(400) has been investigated. It is shown that average cascade curvers calculated in the framework of the QGSJET model for the primary protons with the energy of $10^{18} - 3 \cdot 10^{19}$ eV are in close agreement with experimental datafor EAS with $\theta < 45°$. The absoption path of cascade particles calculated by the same model for inclined EAS describes the experiment worse. A form of the experimental cascade cuver is more sloping than the calculated one. All this requires more careful study of considered both experimental and theoretical questions.

1. Introduction

It is known that the longitudinal and lateral development of EAS is also dependent on themass composition and nuclear interaction peculiarities of primary particles. These characteristics can be studied by such parameters as X_{max}, N_s, N_μ. At present the number of registered showers allow us to analyze the average EAS characteristics in the region of the second bump to a sufficient accuracy. The analysis is the joint consideration of experimental data and theoretical results. In this paper the calculation is carried out by the QGSJET model. This model suggested by Kalmykov et al. (1997) consecutively describes all stages of the nuclear interaction and includes the consideration of semihard processes that allows to obtain the best agreement of calculation results with the experiment especially by the number of muons. In the framework of this model we calculated longitudinal and lateral characteristics of total charged and Cherenkov components of EAS.

2. Methods of Treatment and Analysis of Showers

Because of large separations between observation stations, physical and instrumental fluctuations, some systematic errors in the selection and treatment of showers and also the influence of the geomagnetic field, the determination accuracy of shower parameters and a form of their dependence on the primary energy and the zenith angle are essentially charged. Thus, in showers with $\theta \geq 45°$ a shower front becomes more “loose”, LDFs of different components can change the form. To take into account the above factors we entered an additional parameter $A(\theta,R)$ (Afanasiev et al., 1996) into the minimization procedure which took into account an asymmetry of the charged particles lateral distribution in inclined showers and the array geometry to define the proper value of a core and parameters of a shower. Under a new program, we selected 2400 showers with $N_s \geq 10^8$ particles. For the final analysis 1783 showers were selected the cores of which were in the interior of the array and definition accuracies of shower paramers were $\sigma_\theta = 3\text{ -}5°$, $\sigma_{xy} = (30 \pm 10)$ m, $N_s = (20 - 40)$ % for the big array and measurement accuracies for the small Cherenkov installation (Afanasiev et al.,1997) were $\sigma_\theta = 1\text{ -}3°$, $\sigma_{xy} = (10 \pm 5)$ m, $N_s = (10 - 30)$ %.

3. Results

3.1 Changes of the Paramerter N_s Depending on the Primary Energy and the Zenith Angle

The experimental dependence of N_s on E_O and calculation results by the QGSJET model at different average zenith angles $\langle\theta\rangle$ are presented in Fig.1 and listed in Table 1.

Table 1. Approximation results of experimental and calculated data by a function $N_s=AE^B$

	Experiment			QGSJET model	
n/n	$\langle\theta\rangle$, degs.	A	B	A	B
1	12	-11.8±0.4	1.12±0.02	-11.5±0.3	1.11±0.01
2	20	-12.5±0.4	1.15±0.02		
3	29	-13.8±1.2	1.21±0.06	-13.1±0.2	1.18±0.01
4	38	-16.6±0.3	1.29±0.02	-15.5±0.2	1.29±0.01
5	48	-17.9±0.1	1.39±0.01	-19.2±0.1	1.45±0.01

From Fig.1 and Table 1 it is seen that for vertical showers ($\theta < 30°$) the experimental $N_s^{exp.}$ In absolute magnitude is 20 % less than the calculated one. At $\theta > 45°$ $N_s^{exp.}$ is practically coincident with the theoretical $N_s^{theor.}$. But the difference in the index B of the dependence of N_s on E_O arises as zenith angle increases. Thus, the experimental N_s is reasonably in good agreement with the calculated one except for the most vertical showers, and some difference in the B -index with the increase of the zenith angle is observed. Probably, the absorption of the charged component in real showers with the primary energy increase goes on more slowly than it follows from the QGSJET model.

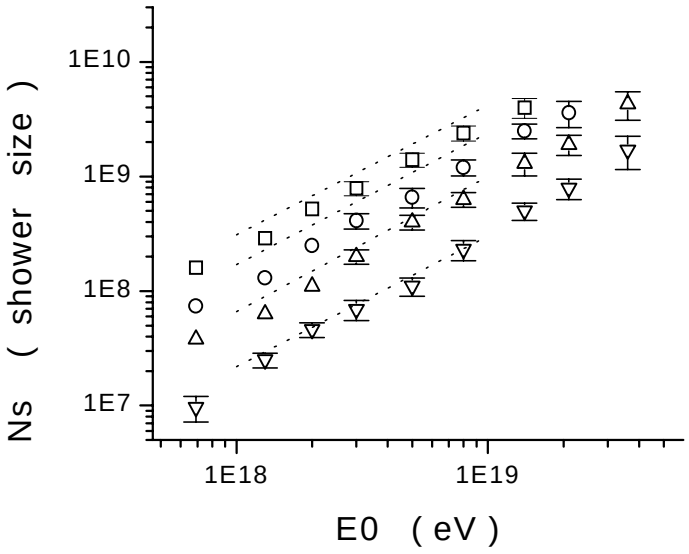

Figure 1. The shower size Ns vs the primary energy for different zenith angles. Experimental data: - $\theta = 12°$, O - $\theta = 29°$, Δ - $\theta = 38°$, ∇ - $\theta = 48°$. Dotted lines are calculated dependences by the QGSJET model

3. The Longitudinal Development of EAS

We constructed experimental curves of the longitudinal EAS development for $E_O = 1.2\cdot10^{18}$, $5\cdot10^{18}$ and $1.2\cdot10^{19}$ eV by the reconstruction method of the cascade curve tail using dependences $N_s \approx f(Q(400))$ in the region of zenith angles $\Delta\theta = 0 - 55°$. The transition to the dependence $N_s - f(E_O)$ was carried out by the formula

$$E_O = (8.9\pm2.6)\cdot10^{17}\cdot Q(400)^{1.03\pm0.02} \qquad (1)$$

and to the dependence $N(x) - f(X_o\cdot \sec\theta)$ - by the section method of curves in Fig.1 for given fixed energies. To compare experimental and theoretical results the points were reduced to the single energy and the atmosphere depth. Fig.2 demonstrates the cascade curves of EAS for the depths

range of 1020 - 1620 g/cm^2 and the curves reduced by the Cherenkov light LDF shape (Dyakonov et al.,1986) from the maximum to sea level.The calculated curves are shown by dotted lines.

From Fig. 2 the difference between experimental and calculated curves with the increase of the atmosphere depth is seen: the experimental curve is more sloping. We analyze absorption path lengths of charged particles for different parts by X (g/cm^2): ΔX_1(1020 - 1320), ΔX_2(1320 - 1620) (see Table 2).

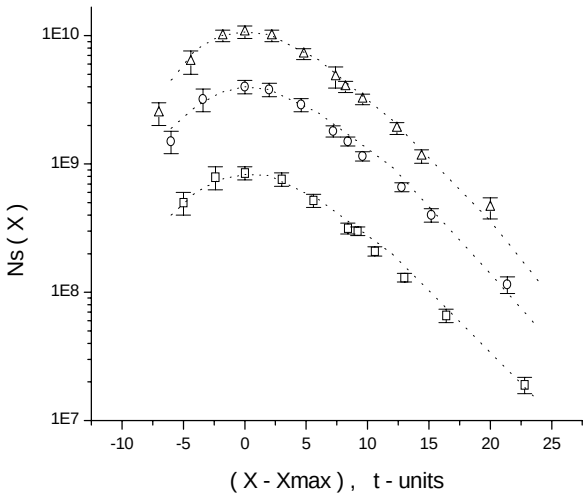

Figure 2. EAS cascade curves.Experimental data: - $E_o = 1{,}2 \cdot 10^{18}$ eV, O - $E_o = 5 \cdot 10^{18}$ eV, Δ - $E_o = 1{,}2 \cdot 10^{19}$ eV. Dotted lines are calculated dependences by the QGSJET model.

Table 2. The absorption path lenghs of charged particles of EAS for different ranges of depths

Experiment				QGSJET model		
$lg_{10}E_o$, eV	18.08	18.70	19.8	18.08	18.70	19.08
$lg_{10}N_s(\theta=12°)$	8.46	9.16	9.58	8.56	9.24	9.70
$\lambda_{abs}(\Delta X_1)$, g/cm^2	187±12	193±14	200±17	178	178	178
$\lambda_{abs}(\Delta X_2)$, g/cm^2	202±20	205±21	215±25	162	164	166

It is evident that absorption path lengths of particles obtained from calculations by the QGSJET model for different ranges of the atmosphere depth are smaller than experimental values. This can be caused by that fact that in calculations he response from γ - quanta was not taken into account and the threshold energy of muons was 0.3 GeV.

3.3 X_{max} - distribution at fixed energies

Consider fluctuations of EAS X_{max} at four fixed energies (see Table 3). The maximum depth was defined by a form of the Cherenkov light lateral distribution, the shower energy by Cherenkov light flux density at R = 100 m and 400 m from a core depending on the shower size. Characteristics of these distributions and also equipment and physical fluctuations of X_{max} are listed in Table 3.

Table 3. Fluctuations of the maximum depth of the shower development

E_o, eV	$\langle X_{max} \rangle$, g/cm^2	$\sigma_{exp.}$, g/cm^2	$\sigma_{inst.}$, g/cm^2	$\sigma_{phys.}$, g/cm^2	m	$\sigma_{QGS.}$, g/cm^2
$5 \cdot 10^{16}$	586±6	81.3±6	55	60±6	323	59±5
$5 \cdot 10^{17}$	654±3	89.4±3	60	66±3	820	60±5
10^{18}	679±3	83.0±3	60	57±3	779	60±5
$5 \cdot 10^{18}$	734±5	88,1±6	65	64±6	464	71±5

From Table 3 it is seen that measured fluctuations of X_{max} at $E_O > 10^{18}$ eV are constant and consistent with values obtained by the QGSJET model for the primary proton within experimental errors.

3.4 Estimation of Inelastic Interaction Cross - Section $\sigma^{prod.}_{p\text{-}air}$

In this work we used the estimation method of $\sigma^{prod.}_{p\text{-}air}$ from a "tail" of the fluctuation distribution of X_{max} (Kalmykov et al., 1993). $\sigma^{prod.}_{p\text{-}air}$ was defined by the formula

$$\sigma^{prod.}_{p\text{-}air}(E) = \langle A \rangle / N_O \cdot \lambda^{in}(E) = 2.41 \cdot 10^4 / \lambda^{in}(E), \text{ mb} \qquad (2)$$

where $\lambda^{in}(E)$ is the interaction path length of a primary particle. $\lambda^{in}_{exp.}(E)$ is defined by the formula: $\lambda^{in}_{exp.}(E) = \Lambda / (k_1 \cdot k_2)$, where Λ is a sloping index in the exponential presentation of the X_{max} distribution "tail", k_1 is a coupling coefficient between $\lambda^{in}_{theor}(E)$ and Λ and it usually depends on the chosen model, k_2 is a correction factor which depends on instrumental errors, in our case on an accuracy in definition of X_{max} equal to ~ 60 g/cm^2. Data on $\sigma^{prod.}_{p\text{-}air}(E)$ for the model are listed in the first column of Table 4.

Table 4. The inelastic interaction cross - sections $\sigma^{prod.}_{p\text{-}air}(E)$

E_o, eV	$\sigma^{prod.}_{theor.}$, mb	$\lambda_{exp.}$, g/cm^2	k_1	k_2	$\lambda_{phys.}$, g/cm^2	$\sigma^{prod.}_{exp.}$, mb
$5 \cdot 10^{16}$	470 ± 3	88.9 ± 9.2	1.4 ± 0.3	1.25	50.8 ± 9.2	474 ± 67
$5 \cdot 10^{17}$	508 ± 3	80.3 ± 8.4	1.4 ± 0.3	1.25	45.9 ± 8.4	525 ± 52
10^{18}	520 ± 3	78.1 ± 8.1	1.4 ± 0.3	1.25	44.6 ± 8.1	540 ± 55
$5 \cdot 10^{18}$	548 ± 3	75,1 ± 7.7	1.4 ± 0.3	1.25	42.9 ± 7.7	562 ± 77

From Table 4 it follows that $\sigma^{prod.}_{theor}(E)$ used in the QGSJET model for the primary proton - air atom nuclei interaction and the experimental value $\sigma^{prod.}_{exp}(E)$ differ from each other insignificantly.

4. Discussion

Experimental data on the longitudinal EAS development obtained at the Yakutsk array for $E_O \geq 10^{18}$ eV are consistent with the calculations by parameters X_{max}, $dX_{max} / d\lg_{10}E$, σX_{max} within experimental errors (except for vertical showers). But there are noticeable difference in absorption path length of EAS particles λ_{abs}. Experimental cascade curves being far removed from their development maximum are decreased more slowly in comparison with calculated ones that can testify to slower development of the real shower as compared with the theoretical one or about the significant contribution of γ-quanta to the charged particle response (scintillation thickness is 5 cm) at large distances from the shower core. This is not taken into account in the calculation. The difference of calculated and experimental X_{max} at $E_O = 5 \cdot 10^{16} - 10^{18}$ eV can be explained if to suggest that the mass composition of primary particles are the mixture of nuclei similar to that which are at the atmosphere boundary at $E_O = 10^{12} - 10^{14}$ eV. At $E_O > 10^{18}$ eV the experimental X_{max} are in better agreement with the calculated ones due to the increase of a portion of protons in primary cosmic rays. Fluctuations and the X_{max} - distribution shape at these energies (see Tables 3 and 4) does not contradict to this conclusion. From Table 4 it also follows that $\sigma^{prod.}_{exp}(E)$ is in good agreement with the approximation of the dependence of $\sigma^{prod.}_{p\text{-}air}$ on the energy which is used in the QGSJET model.

References

Afanasiev B.N. et al. 1996, Proc. ISEHECR, Tokyo, p. 32

Afanasiev B.N. et al. 1997, Proc. 25th ICRC, Durban, v. 7, p. 217

Dyakonov M.N., Knurenko S.P., Kolosov V.A. et al., Nuclear Instruments and Methods in Physics Research, 1986, A248, v. 4, p. 224

Kalmykov N.N. et al.,1993, Izv. RAN, seriya fis., v. 57, p.2

Kalmykov N.N. et al.,1997, Nucl. Phys. B (Proc. Suppl.), 52B, 17